XII International Conference on Computational Plasticity. Fundamentals and Applications
COMPLAS XII
E. Oñate, D.R.J. Owen, D. Peric and B. Suárez (Eds)

A FINITE ELEMENT STRATEGY COUPLING A GRADIENT-ENHANCED DAMAGE MODEL AND COHESIVE CRACKS FOR QUASI-BRITTLE MATERIALS

ELENA TAMAYO-MAS*, **ANTONIO RODRÍGUEZ-FERRAN***

*Laboratori de Càlcul Numèric (LaCàN)
Departament de Matemàtica Aplicada III
Universitat Politècnica de Catalunya
Campus Nord UPC, 08034 Barcelona, Spain
e-mail: {elena.tamayo, antonio.rodriguez-ferran}@upc.edu
web page: http://www.lacan.upc.edu/

Key words: Continuous-discontinuous strategy, regularisation, smoothed displacements, eXtended Finite Element Method, cohesive cracks, medial surface

Abstract. A new combined strategy to describe failure of quasi-brittle materials is presented thus allowing the complete description of the process, from initiation of damage to crack propagation.

For the early stages of the process, and in order to overcome the well-known problems characterising local descriptions of damage (e.g. mesh-dependence), a gradient-enhanced model based on smoothed displacements is employed. In order to deal with material separation, this continuous description is coupled to a cohesive crack when damage parameter exceeds a critical value.

Some difficulties may arise when dealing with the transition from regularised damage models to evolving cracks: crack initiation, crack-path direction, energetic equivalence... In this work, a discrete cohesive crack is introduced when the damage parameter exceeds a critical value. On the one hand, and to determine the crack-path direction, the medial axis of the already damaged profile is computed. That is, a geometric tool widely used in the computer graphics field is used here to track the crack surface. Since this technique is exclusively based on the shape of the regularised damage profile, no mesh sensitivity is observed when determining the crack direction. On the other hand, and to define the cohesive law, an energy balance is imposed thus ensuring that the fracture energy not yet dissipated in the damage zone is transferred to the crack.

1 INTRODUCTION

In order to simulate failure of quasi-brittle materials —concrete, for example— two different points of view can be used: damage and fracture mechanics.

On the one hand, continuous models for failure analysis —damage or softening plasticity— can be used to describe the early stages of the failure process. They are based on a strain-softening phenomenon which leads to an ill-posed problem when the peak in the stress-strain curve is reached. As a consequence, numerical simulations present a pathological mesh sensitivity thus leading to physically unrealistic results. To overcome this physically unrealistic behaviour, different remedies can be found in the literature. One of these possible solutions consists of using a gradient-type formulation [1, 2]. However, despite this regularisation, non-local continuum failure models cannot deal with displacement discontinuities and thus cannot handle cracks.

Furthermore, dealing with material separation and explicitly modelling the crack geometry is suitable for many applications. For instance, in hydraulic fracturing processes —such as magma-driven dykes and fracturing of oil and gas reservoirs— the hydraulic pressure depends on the shape of the crack and in rock fracture mechanics, the explicit simulation of cracks allows to model the permeability for fluid movement.

On the other hand, discontinuous models incorporate discontinuous displacement fields, thus leading to the necessity of dealing with formation and growth of cracks. To characterise these propagating discontinuities, different techniques, mainly based on the cohesive crack concept [3], have been developed. From a numerical viewpoint, as reviewed in [4], special techniques have to be used to deal with propagating cracks, such as the eXtended Finite Element Method (X-FEM) [5,6]. However, as discussed in [7], discontinuous models cannot be used for modelling the first stages of failure, since they are not able to describe neither damage inception nor its diffuse propagation.

As suggested by the above discussion, combining these two theories —damage and fracture— is a way to achieve a better characterisation of the whole failure process. Different contributions in this direction can be found in the literature, see [7–12].

In this paper, a new combined approach is presented. First, an implicit gradient-enhanced continuum model based on smoothed displacements is used to simulate the initial stages of failure. Then, it is coupled to a discontinuous model to capture crack initiation and its propagation. Special emphasis is placed on the transition process. On the one hand, and in order to conserve the energy dissipation through the change of models, an appropriate cohesive law must be defined. On the other hand, the direction of the crack path should be determined. Here, a new strategy is proposed: the discontinuity is propagated following the direction dictated by the medial axis of the damaged domain. That is, a geometric tool, widely used in the computer graphics field, is used here to locate cracks.

1.1 Outline

An outline of this paper follows. The proposed continuous-discontinuous model is presented in Section 2. Firstly, in Section 2.1, the continuous gradient-type formulation is presented. Secondly, in Section 2.2, the coupling to the discontinuous problem fields is described. Section 3 deals with two important issues concerning the transition from the continuum to the discrete strategy: the definition of the cohesive law —Section 3.1— and the determination of the crack path —Section 3.2—. The capabilities of this new technique to locate cracks are illustrated by means of different tests in Section 4. The concluding remarks of Section 5 close the paper.

2 MODEL FORMULATION

2.1 Continuous damage model with smoothed displacements

To simulate the first stages of a failure process, we propose to use an implicit gradient-enhanced continuum model based on smoothed displacements. The idea of this model was presented and illustrated by means of a one-dimensional example in [13]. For the sake of simplicity, here, only scalar damage models are considered. Nevertheless, as discussed in [14], smoothed displacements can be easily extended to a general framework.

In this model, two different displacements are used: (a) the standard or local displacement field $\boldsymbol{u}$ and (b) the gradient-enriched displacement field $\widetilde{\boldsymbol{u}}$, which is the solution of the partial differential equation

$$\widetilde{\boldsymbol{u}}\left(\boldsymbol{x}\right) - \ell^2 \nabla^2 \widetilde{\boldsymbol{u}}\left(\boldsymbol{x}\right) = \boldsymbol{u}\left(\boldsymbol{x}\right) \tag{1}$$

where the diffusion parameter ℓ has the dimension of length.

Hence, the key idea of this alternative formulation is to use this regularised displacement field to drive damage evolution, see Table 1 for details.

Table 1: Gradient damage model based on smoothed displacements.

Constitutive equation	$\boldsymbol{\sigma}\left(\boldsymbol{x}\right) = \left(1 - D\left(\boldsymbol{x}\right)\right) \boldsymbol{C} : \boldsymbol{\varepsilon}\left(\boldsymbol{x}\right)$
Strains	$\boldsymbol{\varepsilon}\left(\boldsymbol{x}\right) = \nabla^s \boldsymbol{u}\left(\boldsymbol{x}\right)$
Smoothed displacements	$\widetilde{\boldsymbol{u}}\left(\boldsymbol{x}\right) - \ell^2 \nabla^2 \widetilde{\boldsymbol{u}}\left(\boldsymbol{x}\right) = \boldsymbol{u}\left(\boldsymbol{x}\right)$
Smoothed strains	$\widetilde{\boldsymbol{\varepsilon}}\left(\boldsymbol{x}\right) = \nabla^s \widetilde{\boldsymbol{u}}\left(\boldsymbol{x}\right)$
Smoothed state variable	$Y\left(\boldsymbol{x}\right) = Y\left(\widetilde{\boldsymbol{\varepsilon}}\left(\boldsymbol{x}\right)\right)$
Damage evolution	$D\left(\boldsymbol{x}\right) = D(Y)$

This alternative formulation requires additional boundary conditions for the smoothed displacement field $\widetilde{\boldsymbol{u}}$. Prescribing boundary conditions at the level of displacements (rather than the internal variable) seems easier to interpret. As discussed in [15], we propose here to use combined boundary conditions —Dirichlet boundary conditions for the normal component of the displacement field and non-homogeneous Neumann boundary conditions for the tangential components—,

$$\left.\begin{array}{rcl}\widetilde{\boldsymbol{u}}\cdot\boldsymbol{n} & = & \boldsymbol{u}\cdot\boldsymbol{n}\\ \nabla\left(\widetilde{\boldsymbol{u}}\cdot\boldsymbol{t}_1\right)\cdot\boldsymbol{n} & = & \nabla\left(\boldsymbol{u}\cdot\boldsymbol{t}_1\right)\cdot\boldsymbol{n}\\ \nabla\left(\widetilde{\boldsymbol{u}}\cdot\boldsymbol{t}_2\right)\cdot\boldsymbol{n} & = & \nabla\left(\boldsymbol{u}\cdot\boldsymbol{t}_2\right)\cdot\boldsymbol{n}\end{array}\right\}\text{on } \partial\Omega \tag{2}$$

where $\boldsymbol{n}$ denotes the outward unit normal to Ω and $\boldsymbol{t}_1$, $\boldsymbol{t}_2$ are tangent vectors such that $\{\boldsymbol{n}, \boldsymbol{t}_1, \boldsymbol{t}_2\}$ form an orthonormal basis for $\mathbb{R}^3$.

2.2 Continuous-discontinuous damage model with smoothed displacements

To simulate the last stages of a failure process, we propose to couple the implicit gradient-enhanced model based on smoothed displacements with propagating cracks.

In this final stage of the process, the bulk Ω is bounded by $\Gamma = \Gamma_u \cup \Gamma_t \cup \Gamma_d$, as shown in Figure 1. Prescribed displacements are imposed on Γ_u, while tractions are imposed on Γ_t. The boundary Γ_d consists of the boundary of the crack.

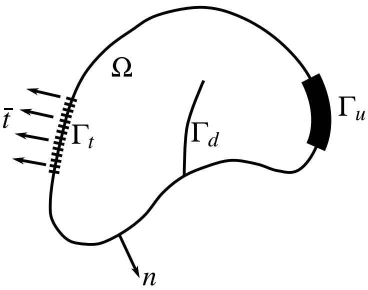

Figure 1: Notations for a body with a crack subjected to loads and imposed displacements.

The key idea of this combined strategy is to characterise the problem fields —both local and non-local displacements— by means of the X-FEM. Indeed, and with X-FEM, $\boldsymbol{u}$ and $\widetilde{\boldsymbol{u}}$ can be decomposed as

$$\boldsymbol{u}(\boldsymbol{x}) = \boldsymbol{u}^1(\boldsymbol{x}) + \psi(\boldsymbol{x})\,\boldsymbol{u}^2(\boldsymbol{x}) \tag{3a}$$

$$\widetilde{\boldsymbol{u}}(\boldsymbol{x}) = \widetilde{\boldsymbol{u}}^1(\boldsymbol{x}) + \psi(\boldsymbol{x})\,\widetilde{\boldsymbol{u}}^2(\boldsymbol{x}) \tag{3b}$$

where $\boldsymbol{u}^i, \widetilde{\boldsymbol{u}}^i$ $(i = 1, 2)$ are continuous fields and ψ is the sign function centred at the discontinuity Γ_d (equals to 1 at one side of the discontinuity and equals to -1 at the other one). Note that, the continuous parts $\boldsymbol{u}^1$ and $\widetilde{\boldsymbol{u}}^1$ correspond to the displacement field without any crack, while the additional discontinuous fields $\psi\boldsymbol{u}^2$ and $\psi\widetilde{\boldsymbol{u}}^2$ model the crack.

In the continuous-discontinuous model with smoothed displacements, the regularisation PDE (1) is employed to incorporate non-locality. Therefore, appropriate boundary conditions for $\widetilde{\boldsymbol{u}}$ must be defined. Here, combined boundary conditions

$$\left.\begin{array}{rcl}\widetilde{\boldsymbol{u}}^i\cdot\boldsymbol{n} & = & \boldsymbol{u}^i\cdot\boldsymbol{n}\\ \nabla\left(\widetilde{\boldsymbol{u}}^i\cdot\boldsymbol{t}_1\right)\cdot\boldsymbol{n} & = & \nabla\left(\boldsymbol{u}^i\cdot\boldsymbol{t}_1\right)\cdot\boldsymbol{n}\\ \nabla\left(\widetilde{\boldsymbol{u}}^i\cdot\boldsymbol{t}_2\right)\cdot\boldsymbol{n} & = & \nabla\left(\boldsymbol{u}^i\cdot\boldsymbol{t}_2\right)\cdot\boldsymbol{n}\end{array}\right\}\text{on }\Gamma \tag{4}$$

where $i = 1, 2$, are prescribed for the continuous displacement fields $\widetilde{\boldsymbol{u}}^1$ and $\widetilde{\boldsymbol{u}}^2$.

3 TRANSITION

The combination of the two traditional approaches —damage and fracture mechanics— enables to obtain a better description of the whole failure process but introduces several difficulties.

3.1 Cohesive model

When introducing a discontinuity in the bulk, the properties of the cohesive crack should be defined. The strategy here used is based on the idea that the energy that would be dissipated by a continuum approach is conserved if a combined strategy is used, see [10, 16].

Consider first the continuous approach and a damaged band λ_D. Then, in this zone of the structure, the dissipated energy can be expressed as

$$\Psi_C = \int_{\lambda_D} \psi_C \,\mathrm{d}\Omega = \int_{\lambda_D}\int_0^{t_f} \boldsymbol{\sigma}_C\cdot\dot{\boldsymbol{\varepsilon}}_C \,\mathrm{d}t\,\mathrm{d}\Omega \tag{5}$$

where the subscript C stands for *Continuous strategy* and $\dot{\boldsymbol{\varepsilon}}_C$ is the strain rate tensor.

Consider now the combined approach. In λ_D, the dissipated energy can be decomposed into two contributions

$$\Psi_{CD} = \Psi_{CD}^{\text{bulk}} + \Psi_{CD}^{\text{crack}} = \int_{\lambda_D}\int_0^{t_f} \boldsymbol{\sigma}_{CD}\cdot\dot{\boldsymbol{\varepsilon}}_{CD}\,\mathrm{d}t\,\Omega + \Psi_{CD}^{\text{crack}} \tag{6}$$

where the subscript CD stands for *Continuous-Discontinuous strategy*, Ψ_{CD}^{bulk} is the dissipated energy of the bulk and Ψ_{CD}^{crack} is the fracture energy.

Therefore, imposing energy balance $\Psi_C = \Psi_{CD}$, the fracture energy

$$\Psi_{CD}^{\text{crack}} = \Psi_C - \Psi_{CD}^{\text{bulk}} \tag{7}$$

is computed and can be transferred to the crack at the moment of the transition.

To estimate the fracture energy, different techniques can be employed. In [10], an analytical estimation of Ψ_{CD}^{crack}, and thus, of the crack stiffness, is computed. Nevertheless, with this procedure, the fracture energy is overestimated. Indeed, by means of these

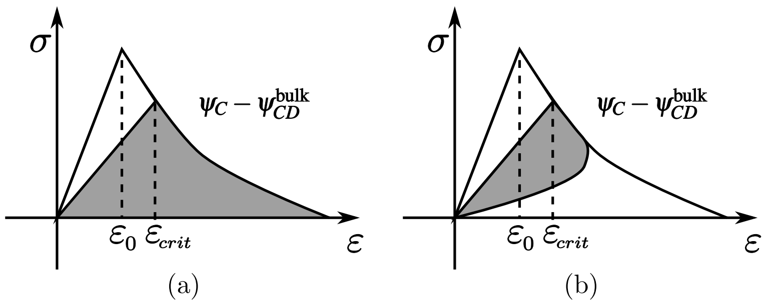

Figure 2: Energy not yet dissipated in the damage band which is transmitted to the cohesive crack and is dissipated by the continuous-discontinuous model, considering that by the continuous strategy, (a) all the points of λ_D download following the softening branch and (b) points of λ_D download following both softening and elastic branches.

assumptions, in all points across the damage band λ_D, the energy $\Psi_C - \Psi_{CD}^{\text{bulk}}$ depicted in Figure 2(a) is transferred to the crack. However, in some of these points, the continuous strategy would dissipate less energy, see Figure 2(b).

As suggested by this discussion, we propose to employ a new strategy which takes into account, for each point across the damage band λ_D, the unloading behaviour (both softening and secant) of the continuous bulk. Since the continuous unloading branch is only known up to the activation of the continuous-discontinuous strategy, we propose to approximate it by the tangent to the transition point. By means of this strategy, the dissipated energy Ψ_{CD}^{crack} is more accurately estimated, although it cannot be exactly computed.

3.2 Direction of crack growth

One important issue concerning the transition from the continuous to the discontinuous approach is the location of a crack and the definition of the direction along which it propagates. Regarding combined approaches, fracture mechanics cannot be employed, since the critical imperfection from which cracking initiates is unknown. Therefore, other criteria should be used.

Traditionally, determining the direction of crack growth is tackled from a mechanical point of view. Here, an alternative way of defining the direction of crack growth is presented. The key idea of this alternative method is to collapse a damaged zone —which can be understood as a crack of thickness equal to the damaged band— into a zero-thickness crack that propagates through the middle of the regularised bulk. This idea —going through the middle of a given domain— can be directly formalised by means of the medial axis concept, a geometric tool widely used in image analysis, see [17].

4 NUMERICAL EXAMPLES

To illustrate the capabilities of this combined approach, two different examples are carried out.

4.1 Three-point bending test

To begin with, a three-point bending test is considered, see Figure 3. The geometric and material parameters are summarised in Table 2. Here, the simplified Mazars damage model [18]

$$Y = \sqrt{\sum_{i=1}^{3} (\max(0, \varepsilon_i))^2} \tag{8}$$

with ε_i ($i = 1, 2, 3$) the principal strains is considered. The exponential damage evolution law

$$D(Y) = 1 - \frac{Y_0}{Y} \exp^{-\beta(Y - Y_0)} \tag{9}$$

is taken into account.

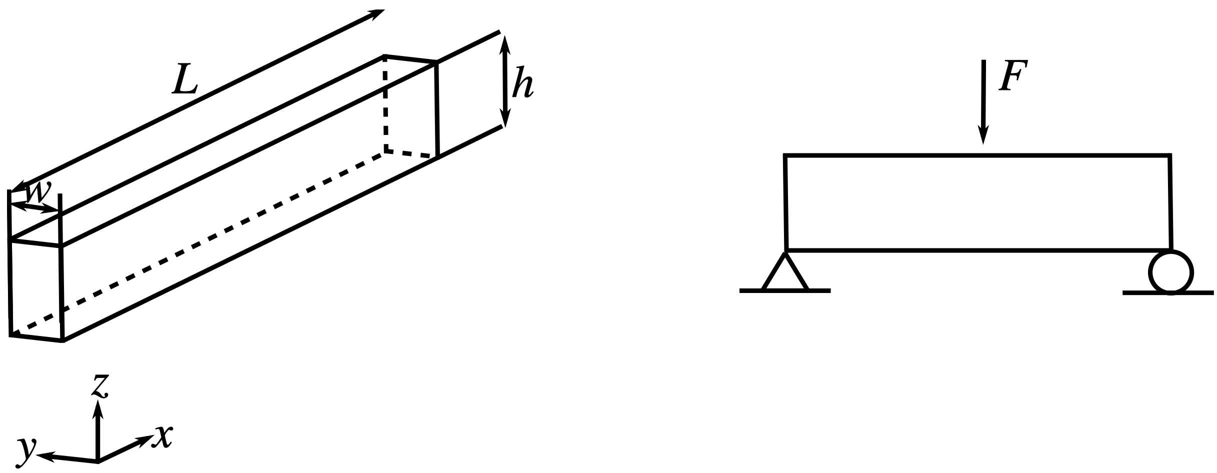

Figure 3: Three-point bending test: problem statement.

Figure 4 shows the obtained results in terms of damage profiles and deformation patterns (amplified by a factor of 100) for some increasing imposed forces F. Firstly, the continuous gradient enhanced damage model with smoothed displacements is used, see Figures 4(a)-4(b); as soon as damage exceeds a critical value, a propagating crack is introduced, see Figures 4(c)-4(f). The simplified medial surface allows to locate the crack where expected.

Table 2: Three-point bending test: geometrical and material parameters.

Meaning	Symbol	Value
Length of the beam	L	3 mm
Height of the beam	h	1 mm
Young's modulus	E	30 000 MPa
Damage threshold	Y_0	10^{-4}
Slope of the stress-strain relation	β	121.93
Poisson's ratio	ν	0.00
Characteristic length	ℓ	0.01 mm

4.2 Four-point bending beam

As a second example, the four-point bending beam numerically analysed in [19] is reproduced, see Figure 5. In view of the central symmetry of the problem, only one half of the specimen has been discretised. The material parameters are summarised in Table 3.

Here, the truncated Rankine damage model,

$$\tau = \sum_{i=1}^{3} \max(0, \tau_i) \tag{10}$$

with τ_i $(i = 1, 2, 3)$ the principal effective stresses with an exponential damage evolution law

$$D(\tau) = 1 - \frac{\tau_0}{\tau} \exp^{-\frac{2H}{\tau_0}(\tau - \tau_0)} \tag{11}$$

is considered.

Table 3: Four-point bending beam: material parameters.

Meaning	Symbol	Value
Young's modulus	E	30 GPa
Damage threshold	τ_0	2 MPa
Fracture energy	G	100 J/m^2
Poisson's ratio	ν	0.2
Characteristic length	ℓ	0.3 cm
Softening parameter	H	8.1×10^{-3}

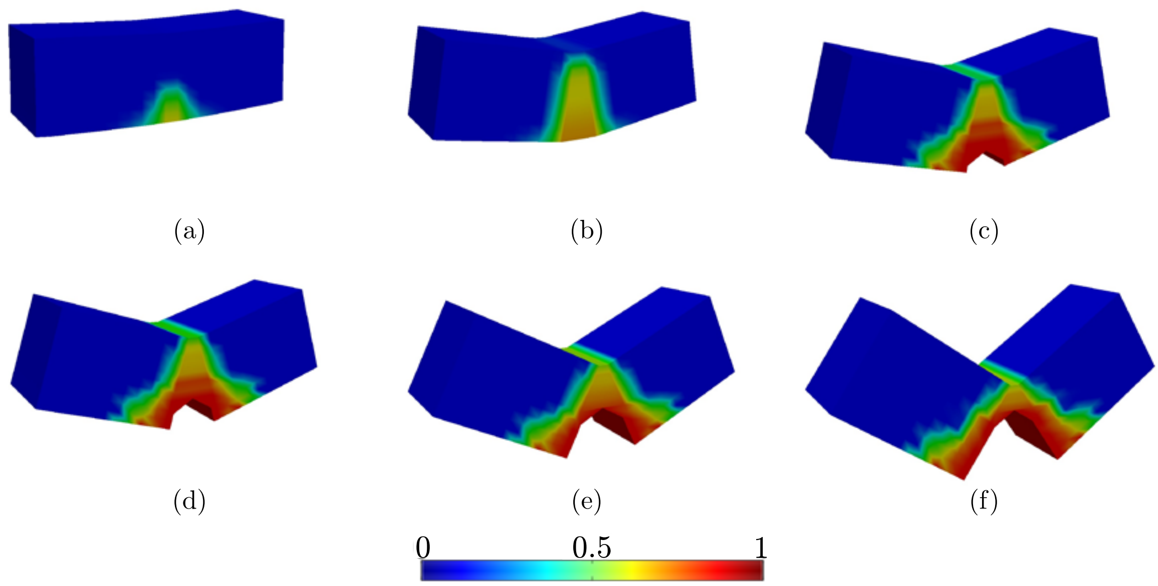

Figure 4: Three-point bending test, CD approach: for increasing imposed force F, damage profiles and deformed meshes ($\times$ 100).

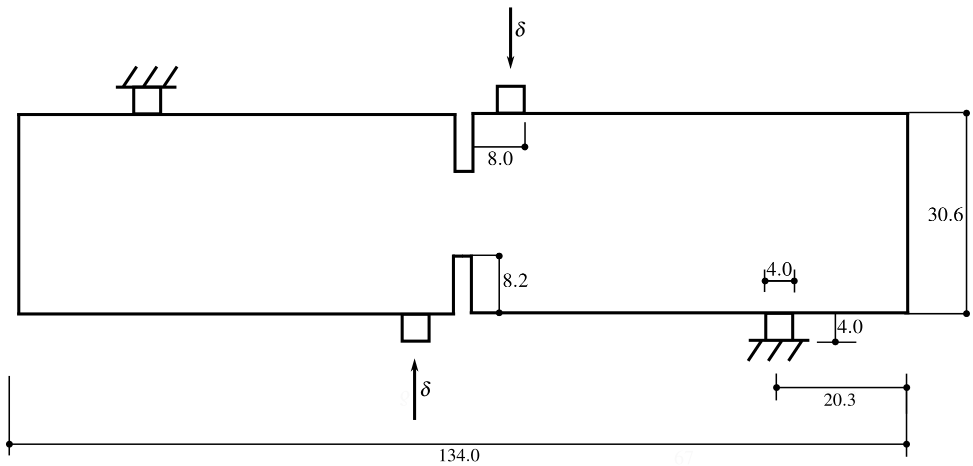

Figure 5: Four-point bending beam: problem statement (measures in centimetres).

For some increasing imposed displacements δ, damage profiles and deformation patterns (amplified by a factor of 100) are shown in Figure 6. As seen, the continuous gradient enhanced damage model with smoothed displacements is used for the first stages of the process, Figures 6(a)-6(b). As soon as a critical situation is achieved, a crack that propagates through the middle of the regularised bulk is introduced, see Figures 6(c)-6(f).

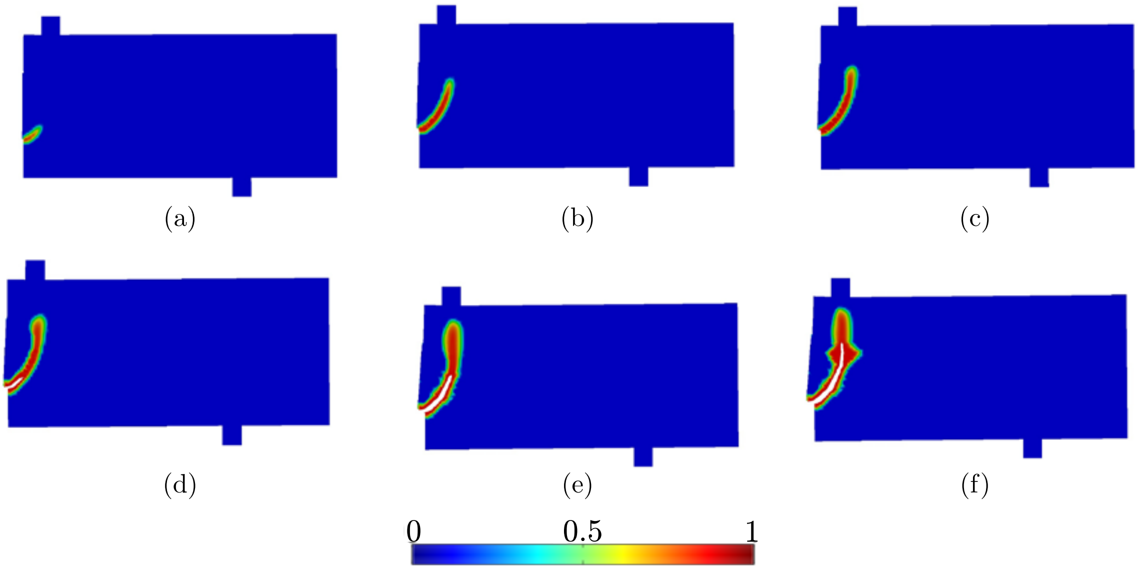

Figure 6: Four-point bending test, CD approach: for increasing imposed displacements δ, damage profiles and deformed meshes ($\times$ 100).

5 CONCLUDING REMARKS

A combined formulation to simulate quasi-brittle failure is proposed. It couples a gradient-enriched formulation with an extended finite element approach. The main features of this new continuous-discontinuous strategy are summarised here:

- To simulate the first stages of the process, an implicit gradient-enhanced continuous model based on smoothed displacements is used.
- Once the transition criterion is fulfilled, a propagating crack is introduced. In order to characterise the discontinuity, the eXtended Finite Element Method is used.
- Special emphasis should be placed on the transition process.
  - Regarding the definition of the cohesive law, an energy balance is prescribed. Hence, the energy that would be dissipated by a continuum approach is conserved.
  - Regarding the direction of the crack-growth a geometric criterion is proposed. Here, the evolving crack propagates following the direction dictated by the medial axis of the damage profile. Since the damaged bulk is regularised and X-FEM is used, the crack path is completely independent of the finite element mesh.

REFERENCES

[1] de Borst, R., Pamin, J., Peerlings, R.H.J. and Sluys, L.J. On gradient-enhanced damage and plasticity models for failure in quasi-brittle and frictional materials. *Computational Mechanics* (1995) **17**:130–141.

[2] Peerlings, R.H.J., de Borst, R., Brekelmans, W.A.M. and Geers, M.G.D. Gradient-enhanced damage modelling of concrete fracture. *Mechanics of Cohesive-frictional Materials* (1998) **3**:323–342.

[3] Hillerborg, A., Modeer, M. and Petersson, P.E. Analysis of crack formation and crack growth in concrete by means of fracture mechanics and finite elements. *Cement and Concrete Research* (1976), **6**:773–781.

[4] Jirásek, M. and Belytschko, T. Computational resolution of strong discontinuities. In *Proceedings of Fifth World Congress on Computational Mechanics, WCCM V, Vienna University of Technology, Austria*, 2002.

[5] Belytschko, T. and Black, T. Elastic crack growth in finite elements with minimal remeshing. *International Journal for Numerical Methods in Engineering* (1999) **45**:601–620.

[6] Moës, N., Dolbow, J. and Belytschko, T. A finite element method for crack growth without remeshing. *International Journal for Numerical Methods in Engineering* (1999) **46**:131–150.

[7] Mazars, J. and Pijaudier-Cabot, G. From damage to fracture mechanics and conversely: A combined approach. *International Journal of Solids and Structures* (1996) **33**:3327–3342.

[8] Jirásek, M. and Zimmermann, T. Embedded crack model. Part II: combination with smeared cracks. *International Journal for Numerical Methods in Engineering* (2001) **50**:1291–1305.

[9] Simone, A., Wells, G. N. and Sluys, L. J. From continuous to discontinuous failure in a gradient-enhanced continuum damage model. *Computer Methods in Applied Mechanics and Engineering* (2003) **192**:4581–4607.

[10] Comi, C., Mariani, S. and Perego, U. An extended FE strategy for transition from continuum damage to mode I cohesive crack propagation. *International Journal for Numerical and Analytical Methods in Geomechanics* (2007) **31**:213–238.

[11] Benvenuti, E. and Tralli, A. Simulation of finite-width process zone in concrete-like materials by means of a regularized extended finite element model. *Computational Mechanics* (2012) **50**:479–497.

[12] Cuvilliez, S., Feyel, F., Lorentz, E. and Michel-Ponnelle, S. A finite element approach coupling a continuous gradient damage model and a cohesive zone model within the framework of quasi-brittle failure. *Computer Methods in Applied Mechanics and Engineering* (2012) **237–240**:244–259.

[13] Rodríguez-Ferran, A., Morata, I. and Huerta, A. A new damage model based on nonlocal displacements. *International Journal for Numerical and Analytical Methods in Geomechanics* (2005) **29**:473–493.

[14] Rodríguez-Ferran, A., Bennett, T., Askes, H. and Tamayo-Mas, E. A general framework for softening regularisation based on gradient elasticity. *International Journal of Solids and Structures* (2011) **48**:1382–1394.

[15] Tamayo-Mas, E. and Rodríguez-Ferran, A. Condiciones de contorno en modelos de gradiente con desplazamientos suavizados. *Revista Internacional de Métodos Numéricos para Cálculo y Diseño en Ingeniería* (2012) **28**:170–176.

[16] Cazes, F., Coret, M., Combescure, A. and Gravouil, A. A thermodynamic method for the construction of a cohesive law from a nonlocal damage model. *International Journal of Solids and Structures* (2009) **46**:1476–1490.

[17] Blum, H. A transformation for extracting new descriptors of shape. *Models for the perception of speech and visual form* (1967) **19**:362–380.

[18] Mazars, J. A description of micro- and macroscale damage of concrete structures. *Engineering Fracture Mechanics* (1986) **25**:729–737.

[19] Cervera, M., Chiumenti, M. and Codina, R. Mesh objective modeling of cracks using continuous linear strain and displacement interpolations. *International Journal for Numerical Methods in Engineering* (2011) **87**:962–987.